PHYSICAL REVIEW B **83**, 020101(R) (2011)

Angular dispersion of oblique phonon modes in $BiFeO_3$ from micro-Raman scattering

J. Hlinka,[1,*] J. Pokorny,[2] S. Karimi,[2] and I. M. Reaney[2]

[1]*Institute of Physics, Academy of Sciences of the Czech Republic, Na Slovance 2, 182 21 Prague 8, Czech Republic*

[2]*Department of Engineering Materials, University of Sheffield, Sheffield S1 3JD, United Kingdom*

(Received 5 November 2010; published 10 January 2011)

The angular dispersion of oblique phonon modes in a multiferroic $BiFeO_3$ has been obtained from a micro-Raman spectroscopic investigation of a coarse grain ceramic sample. Continuity of the measured angular dispersion curves allows conclusive identification of all pure zone-center polar modes. The method employed here to reconstruct the anisotropic crystal property from a large set of independent local measurements on a macroscopically isotropic ceramic sample profits from the considerable dispersion of the oblique modes in ferroelectric perovskites and it can be in principle conveniently applied to any other optically uniaxial ferroelectric material.

DOI: 10.1103/PhysRevB.83.020101 PACS number(s): 77.22.Gm, 77.80.−e, 63.20.D−, 75.80.+q

The discovery of ferroelectric polarization (100 C/cm^2) coexisting with robust magnetic order in $BiFeO_3$ has prompted the recent revival of research into magnetoelectric multiferroics and has led to new ideas for their potential applications. $BiFeO_3$ has become the archetype multiferroic model system.[1–3] With several hundreds of new publications in the past few years, understanding of its physical properties has been considerably improved.[1,3] It is now well established that bulk $BiFeO_3$ is ferroelectric up to ∼1100 K (T_C) and that it possesses an incommensurately modulated G-type canted antiferromagnetic spin structure up to ∼640 K (T_N). At room temperature it has a rhombohedrally distorted structure with R3c symmetry, which can be derived from a standard cubic ABO_3 perovskite by simultaneous polar cation displacement, anticlockwise rotations of neighboring oxygen octahedra, and an elongation of the unit cell along common $[111]_c$ direction of the parent cubic phase.

The Brillouin zone center normal modes of such a crystal structure can be classified into $4A_1 \oplus 5A_2 \oplus 9E$ irreducible representations. The simultaneously IR and Raman active A_1 and E modes are polarized along and perpendicularly to the polar axis ($[111]_c$ pseudocubic direction) while A_2 modes are nonpolar and silent. Information about the frequencies of polar phonon modes is one of the basic ingredients for quantitative insight in dielectric and electromechanical properties of $BiFeO_3$.

In principle, when working with single-domain crystals, polarized light spectroscopies allow probing of optic modes of separate irreducible representations. Recently, a number of $BiFeO_3$ samples have been intensively investigated by IR reflectivity[4–8] and Raman scattering[9–22] techniques. Most notably, the authors of Ref. 5 showed that a $BiFeO_3$ (BFO) single crystal with a large $(100)_c$ surface allowed the probing of near-normal reflectivity for IR light polarized perpendicular to the spontaneous polarization. The low-temperature spectra of Ref. 5 showed exactly the nine expected polar modes belonging to the E symmetry. However, the available crystal surface did not allow measurements of reflectivity of IR light parallel to the spontaneous polarization and there is no convincing evidence for the set of all four transversal optic (TO) and four longitudinal optic (LO) frequencies of A_1 modes of $BiFeO_3$. The assignments of the published (mostly Raman) spectra are mutually conflicting and sometimes even disagree with the results of IR reflectivity from Ref. 5.

The major difficulty in the assignment of individual Raman spectra of $BiFeO_3$ and other ferroelectric crystals is the existence of the so-called *oblique* phonon modes, which, as a rule, do not transform according to the zone-center mode irreducible representations and for which the mode frequency continuously varies with the direction of the phonon propagation vector with respect to the crystallographic axes in the probed volume of the crystal. To clarify this point, we have experimentally determined the angular dependence of long-wavelength polar phonon mode frequencies in $BiFeO_3$ as a function of the phonon propagation vector orientation, hereafter called *angular dispersion*. Simultaneously, our experiments provide a complete list of the pure zone-center polar modes of $BiFeO_3$, which may serve as consistent experimental reference for comparison with density functional theory (DFT) based computations.[23,24]

Angular dispersions can be obtained as square roots of the eigenvalues of the dynamical matrix

$$M_{ij} = \omega_{\mathrm{TO}i}^2 \delta_{ij} + \Omega_i \Omega_j (\mathbf{p_i} \cdot \mathbf{q})(\mathbf{p_j} \cdot \mathbf{q}), \qquad (1)$$

where $\omega_{\mathrm{TO}i}$ is the TO mode frequency, $\mathbf{q}$ is the unit vector parallel to the phonon propagation wave vector, and $\mathbf{p_i}$ is a unit vector directed along the polarization of the mode i. The screened plasma frequency vectors $\mathbf{\Omega_i}$ of the ith TO mode can be obtained from the full set of TO and LO mode frequencies as, for example, in Ref. 27. The index i should go through all independent components of all zone center polar optic modes in the crystal, but for optically uniaxial crystals the equation has rotational symmetry so that it is convenient to exclude the purely transverse components of E(TO) modes.

In optically uniaxial crystals like $BiFeO_3$, only the angle ϕ is relevant, which lies between the phonon propagation vector $\mathbf{q}$ and the optical axis $\mathbf{z}_r$, parallel to the spontaneous ferroelectric polarization. The angular dispersion calculated with the help of TO and LO frequencies taken from the DFT data from Ref. 23 is shown in Fig. 1(a). There are 9 pure E(TO) modes, which can propagate at any angle ϕ at the same frequency (dashed lines). In addition, there are 13 branches of dispersive oblique modes, connecting $9E(\mathrm{TO}) \oplus 4A_1(\mathrm{LO})$ modes at $\phi = 0$ to the $9E(\mathrm{LO}) \oplus 4A_1(\mathrm{TO})$ modes at $\phi = \pi/2$ (full lines). As a result, at $\phi = 0$, the 22 distinct polar mode branches merge to only 13 distinct frequencies at $\phi = 0$.

Measurements of such angular dispersions normally require demanding Raman scattering experiments and de-twinned

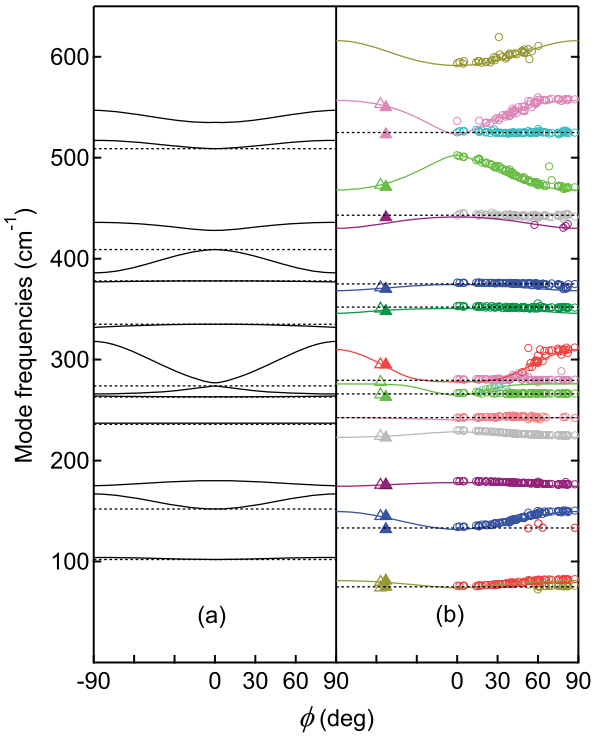

FIG. 1. (Color online) Angular phonon dispersion curves of $BiFeO_3$. Continuous lines are evaluated by diagonalization of the matrix defined in Eq. (1) with TO and LO frequencies (a) taken from DFT data of Ref. 23 and (b) adjusted to present Raman data (as explained in the text). Full lines stand for dispersive oblique modes, dashed lines for the purely transverse E(TO) branches. Open circles are values of the fitted DHO frequencies from individual Raman spectra as a function of the angle ϕ determined from Eq. (2). Full and open triangles stand for the Raman frequencies from Fig. 1. of Refs. 9 and, 10 respectively (1 cm^{-1} = 29.979 245 8 GHz).

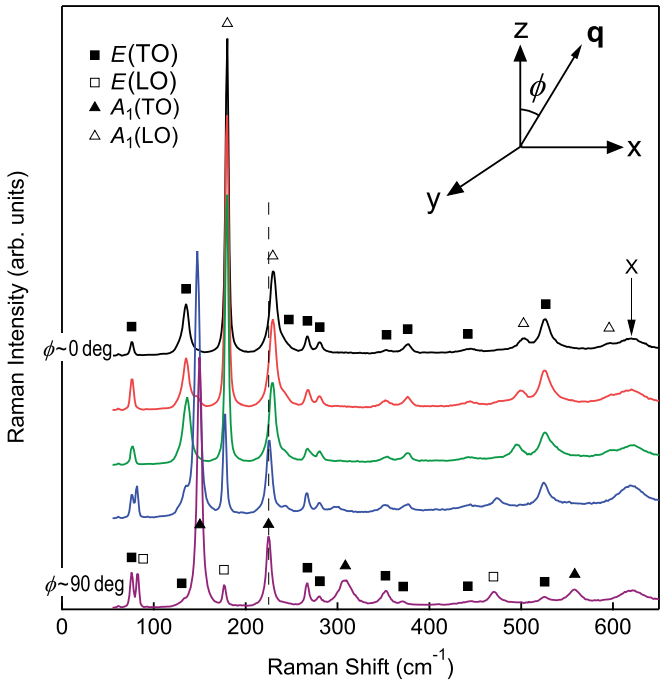

FIG. 2. (Color online) Raman spectra from selected grains of the investigated $BiFeO_3$ ceramics. Top and bottom spectra correspond to grains with their optical axes almost parallel and almost perpendicular to the incident laser beam, respectively. Point symbols indicate positions of the TO and LO frequencies of the pure A_1 and E modes.

single crystals. So far they have been completed for a few materials only (e.g., $BaTiO_3$, $PbTiO_3$, $Sn_2P_2S_6$).[25–27] The growing of $BiFeO_3$ crystals is difficult, but the angular dispersions may be also obtained with the help of a conventional micro-Raman spectrometer and a coarse-grain ceramic pellet. In particular, the present experiment was carried out with an air-sintered (3h, 1100 K) $BiFeO_3$ ceramic sample prepared from high-purity chemicals as described previously in Ref. 32. A Renishaw InVia micro-Raman spectrometer was operated with a 514-nm Ar laser beam focused on an ~2-μm spot in a usual backscattering geometry. The spectra were collected from an unpolished surface of an as-sintered pellet at ~80 K to reduce thermal broadening of the phonon lines.

Measurements were taken from 70 randomly selected individual grains having a well-developed (5–20 μm) regular facet oriented perpendicular to the incident laser beam. Typical spectra are shown in Fig. 2 and are similar to those published earlier. Apart from the first-order Raman lines, they also show a broad band near 620 cm^{-1} which we shall discuss separately. All spectra were fitted according to a standard procedure to a sum of individual damped harmonic oscillator (DHO) response functions multiplied by the Bose–Einstein thermal factor. The DHO frequencies of certain phonon lines were drifting when going from grain to grain, suggesting directly that these are associated with the dispersive, oblique modes (e.g, the mode near the dashed vertical line in Fig. 2). The individual spectra were then sorted according to the decreasing frequency of the oblique mode near the dashed vertical line (~220 cm^{-1}). Since the dispersion curves of oblique modes are monotonous functions of the (0–$\pi/2$) interval of the angle ϕ, the first and the last spectrum should correspond to the angle $\phi \sim 0$ and $\pi/2$ or vice versa.[28]

Since the first spectrum in the ordered series (shown as the top one in Fig. 2) has only 13 phonon lines, it must be the $\phi \sim 0$ spectrum, where only $9E(\mathrm{TO}) \oplus 4A_1(\mathrm{LO})$ modes contribute. Nine of the modes correspond to the $9E$(TO) frequencies identified[5] in the IR reflectivity spectra. Therefore, we can safely conclude that the 4 remaining modes are the A_1(LO) singlets. The subsequent spectra should correspond to higher and higher values of ϕ. The E(TO) modes are split into one (nondispersive) purely TO branch and one (dispersive) branch of oblique modes, as clearly observed for the lowest frequency doublet shown in Fig. 2. Therefore, the last spectrum (bottom of Fig. 2) should correspond to the $\phi \sim \pi/2$ where $9E(\mathrm{TO}) \oplus 9E(\mathrm{LO}) \oplus 4A_1(\mathrm{LO})$ contribute. After the elimination of the E-symmetry modes by comparison with the frequencies determined by the IR experiment in Ref. 5, there are only 4 bands left corresponding to the 4 expected A_1(TO) modes. The list of the 26 LO and TO mode frequencies obtained from our experiment is given in Table I.

The angular dispersion calculated from the set of 13 TO + 13 LO mode frequencies determined in our experiment is

TABLE I. The list of the 26 TO and LO polar mode frequencies of $BiFeO_3$ (in cm^{-1}, at 80 K) as obtained in the present work. Numbers in parentheses are plasma frequencies $\Omega_i = |\mathbf{\Omega_i}|$.

Mode	E(TO)	E(LO)	A_1(TO)	A_1(LO)
1	74 (291)	81	149 (574)	178
2	132 (717)	175	223 (268)	229
3	240 (309)	242	310 (1177)	502
4	265 (970)	276	557 (304)	591
5	278 (421)	346		
6	351 (228)	368		
7	374 (269)	430		
8	441 (205)	468		
9	523 (537)	616		

shown by the continuous lines in Fig. 1(b). Since certain oblique phonon branches have a considerable dispersion, comparison of the measured phonon frequencies with the calculated dispersion may be used to determine the angle ϕ. To facilitate this task, we have determined numerically a formula approximating the inverse function to the 4th lowest oblique dispersion curve[29] $\omega_4(\phi)$ in the form

$$\phi = \left[\arccos\left(\frac{\omega_4^2 - \omega_{\min}^2}{\Delta}\right)\right]^{\beta}, \qquad (2)$$

where $\omega_{\min} \doteq 223\ cm^{-1}$, $\Delta \doteq 2250\ cm^{-2}$, and $\beta \doteq 2/3$. The angle ϕ was assigned to a given spectrum by inserting the fitted value of the phonon frequency ω_4 in this spectrum (the oblique mode near 220 cm^{-1}) into Eq. (2). Finally, by plotting all mode frequencies as a function of the angle ϕ (open circles in the right part of the figure), the full angular phonon dispersion was reconstructed. The agreement between the calculated branches and the full set of recorded data visibly confirms the internal consistency of our approach.

In the adopted backscattering geometry, the angle ϕ discussed previously is between the rhombohedral axis of the studied grain and the incident laser beam. It is known that the angle ψ between the laser beam polarization and the projection of the rhombohedral axis in the plane perpendicular to incident laser beam may be determined from the Raman intensity variations, as shown in, for example, Ref. 11. Thus, in principle, a single Raman spectrum may allow the complete determination of the orientation of the rhombohedral axis of the investigated grain.

The oblique mode dispersion curves determined in this work also allow understanding of the inconsistencies between assignments of the recently reported $BiFeO_3$ Raman spectra. For example, the Raman spectra of a single-domain crystal investigated in Ref. 9 were taken from the $(100)_c$ surface, so that the angle ϕ was close to 54°. Indeed, the mode frequencies from Table I of Ref. 9 coincide with our calculation for this particular angle (data of Ref. 9 are shown in Fig. 1(b) by full triangle symbols.) It thus becomes apparent that the frequencies of 553, 473, and 295.2 cm^{-1} originally assigned as E(TO) modes are actually oblique modes that do not match any pure TO or LO mode frequency. The same new explanation holds for the 550, 471, and 295 cm^{-1} modes, assigned originally[10] as E(TO), A_1(LO), and E(TO) modes, respectively. Interestingly, the assignment of the single-domain Raman spectra of Ref. 12, taken in the "proper" geometry allowing nominally only scattering by phonons propagating along the optical axis, appears also to be misled by oblique modes: the frequency at 147 cm^{-1}, assigned to the lowest A_1 mode, is probably an oblique mode with ϕ of 71°, arising due to ferroelastic twinning.

The disregarded Raman band near 620 cm^{-1} is anomalous not only by its considerable broadness, but also by the independence of its frequency and intensity on the angle ϕ. In agreement with the previous works, it was not included among the regular zone center phonon modes. Interestingly, its frequency is about one-half of the strong band near 1250 cm^{-1}, earlier assigned as a two-phonon band.[9,13] Therefore, its assignment deserves broader discussion in the context of the other magnon and two-phonon Raman scattering bands[30,31] but this is beyond the scope of this work.

Surprisingly, the experimental results are only in qualitative agreement with the predictions of recent DFT calculations.[23,24] For example, we confirm that the third A_1(TO) mode has the largest plasma frequency. On the other hand, the lowest frequency A_1(TO) mode has larger frequency than the second A_1(TO) mode in the experiment but in the calculations of Ref. 23 it is not like that. Also, the plasma frequencies of E(TO) modes suggest that our 4th E(TO) mode actually corresponds to the 5th E(TO) mode in the DFT spectrum.[23] Interestingly, phonon frequencies predicted for $BiFeO_3$ have been found to be highly sensitive to the differences among the currently used DFT implementations,[23,24] implying that comparison with experiment is needed.[24]

In conclusion, we have been able to unambiguously identify frequencies of all polar phonon modes of $BiFeO_3$ by micro-Raman scattering from a coarse-grain ceramic sample. To achieve this goal, we have taken advantage of the focusing possibilities and enhanced signal throughput of current micro-Raman spectrometers and employed a strategy in which the lack of single-domain single crystals is compensated by the possibility to collect a large number of spectra from randomly oriented crystalline grains. In addition, we have indicated how the obtained information can be used to find orientation of the rhombohedral axis in individual grains or ferroelastic domains of $BiFeO_3$. The experimental protocol and analysis employed here is quite general and it can be applied to other optically uniaxial crystals. The agreement between the experiment and the state-of-the-art DFT calculations for polar mode spectrum in $BiFeO_3$ is only qualitative and calls for further investigation.

This work was supported by EPSRC Grant No. EP/H048049/1 and by Project GACR P204/10/0616.

*hlinka@fzu.cz

[1] G. Catalan and J. F. Scott, Adv. Mater. **21**, 2463 (2009).

[2] R. Ramesh and N. A. Spaldin, Nat. Mater. **6**, 21 (2007).

[3] J. Kreisel, B. Noheda, and B. Dkhil, Phase Transitions **82**, 633 (2009).

[4]S. Kamba, D. Nuzhnyy, M. Savinov, J. Sebek, J. Petzelt, J. Prokleska, R. Haumont, and J. Kreisel, Phys. Rev. B **75**, 024403 (2007).

[5]R. P. S. M. Lobo, R. L. Moreira, D. Lebeugle, and D. Colson, Phys. Rev. B **76**, 172105 (2007).

[6]G. A. Komandin, V. I. Torgashev, A. A. Volkov, O. E. Porodinkov, I. E. Spektor, and A. A. Bush, Phys. Solid State **52**, 734 (2010).

[7]R. Haumont, P. Bouvier, A. Pashkin, K. Rabia, S. Frank, B. Dkhil, W. A. Crichton, C. A. Kuntscher, and J. Kreisel, Phys. Rev. B **79**, 184110 (2009).

[8]J. Lu, M. Schmidt, P. Lunkenheimer, A. Pimenov, A. A. Mukhin, V. D. Travkin, and A. Loidl, J. Phys. Conf. Ser. **200**, 012106 (2010).

[9]R. Palai, H. Schmid, J. F. Scott, and R. S. Katiyar, Phys. Rev. B **81**, 064110 (2010); **81**, 139903(E) (2010).

[10]M. Cazayous, D. Malka, D. Lebeugle, and D. Colson, Appl. Phys. Lett. **91**, 071910 (2007).

[11]A. A. Porporati, K. Tsuji, M. Valant, A.-K. Axelsson, and G. Pezzotti, J. Raman Spectrosc. **41**, 84 (2009).

[12]H. Fukumura, H. Harima, K. Kisoda, M. Tamada, Y. Noguchi, and M. Miyayama, J. Magn. Magn. Mater. **310**, e367 (2007).

[13]M. Cazayous, A. Sacuto, D. Lebeugle, and D. Colson, Eur. Phys. J. B **67**, 209 (2009).

[14]R. Palai, R. S. Katiyar, H. Schmid, P. Tissot, S. J. Clark, J. Robertson, S. A. T. Redfern, G. Catalan, and J. F. Scott, Phys. Rev. B **77**, 014110 (2008).

[15]R. Haumont, J. Kreisel, and P. Bouvier, Phase Transitions **79**, 1043 (2006).

[16]D. Rout, K.-S. Moon, and S.-J. L. Kang, J. Raman Spectrosc. **40**, 618 (2009).

[17]M. K. Singh, S. Ryu, and H. M. Jang, Phys. Rev. B **72**, 132101 (2005).

[18]M. N. Iliev, M. V. Abrashev, D. Mazumdar, V. Shelke, and A. Gupta, Phys. Rev. B **82**, 014107 (2010).

[19]G. L. Yuan, S. W. Or, and H. L. W. Chan, J. Phys. D **40**, 1196 (2007).

[20]R. Haumont, J. Kreisel, P. Bouvier, and F. Hippert, Phys. Rev. B **73**, 132101 (2006).

[21]H. Bea, M. Bibes, S. Petit, J. Kreisel, and A. Barthelemy, Philos. Mag. Lett. **87**, 165 (2007).

[22]P. Rovillain, M. Cazayous, Y. Gallais, A. Sacuto, R. P. S. M. Lobo, D. Lebeugle, and D. Colson, Phys. Rev. B **79**, 180411 (2009).

[23]P. Hermet, M. Goffinet, J. Kreisel, and Ph. Ghosez, Phys. Rev. B **75**, 220102(R) (2007).

[24]M. Goffinet, P. Hermet, D. I. Bilc, and Ph. Ghosez, Phys. Rev. B **79**, 014403 (2009).

[25]C. M. Foster, Z. Li, M. Grimsditch, S. K. Chan, and D. J. Lam, Phys. Rev. B **48**, 10160 (1993).

[26]T. Nakamura, S. Kojima, M. S. Jang, M. Takashige, and S. Itoh, J. Phys. Colloques **42**, C6-418 (1981).

[27]J. Hlinka, I. Gregora, and V. Vorlicek, Phys. Rev. B **65**, 064308 (2002).

[28]The few data points scattered from the continuous branches correspond to weak spectral features, most likely arising from adjacent grains or ferroelastic domains.

[29]This branch was selected because the associated spectral band was well isolated from other modes. The difference between our approximative formula (2) and the exact profile obtained numerically by inverting Eq. (1) is negligible.

[30]M. O. Ramirez, M. Krishnamurthi, S. Denev, A. Kumar, S.-Y. Yang, Y.-H. Chu, E. Saiz, J. Seidel, A. P. Pyatakov, A. Bush, D. Viehland, J. Orenstein, R. Ramesh, and V. Gopalan, Appl. Phys. Lett. **92**, 022511 (2008).

[31]M. O. Ramirez, A. Kumar, S. A. Denev, Y. H. Chu, J. Seidel, L. W. Martin, S.-Y. Yang, R. C. Rai, X. S. Xu, J. F. Ihlefeld, N. J. Podraza, E. Saiz, S. Lee, J. Klug, S. W. Cheong, M. J. Bedzyk, O. Auciello, D. G. Schlom, J. Orenstein, R. Ramesh, J. L. Musfeldt, A. P. Litvinchuk, and V. Gopalan, Appl. Phys. Lett. **94**, 161905 (2009).

[32]S. Karimi, I. M. Reaney, Y. Han, J. Pokorny, and I. Sterianou, J. Mater. Sci. **44**, 5102 (2009).